Friction factors of finite and infinite square arrays of roughened pins

D. Wilkie*

Friction factors of square arrays of roughened pins in smooth channels have been measured for a range of pin pitch to diameter ratios and roughness heights and for different sizes of array. The influence of the smooth channel has been removed in two ways; by extrapolating the results for a fixed pitch-to-diameter ratio to an infinite number of pins and by calculation from the finite array results. The resultant friction factors are compared with each other and with data obtained by testing single pins in smooth circular channels and transforming by various methods to the fully rough situation.

Keywords: *fluid flow, friction factor, roughened surfaces, square array*

To obtain heat transfer and friction factor data on roughened surfaces for application to gas-cooled nuclear reactor fuel element clusters it has been customary, for convenience and simplicity and for reasonable representation of the cluster configuration, to test single roughened pins in smooth circular channels and apply a transformation method to separate the heat transfer and friction factor data of the pin from those of the channel. The original Hall transformation[1] depended on time-consuming measurements of velocity and temperature profiles. The velocity profile was used to locate the maximum velocity which, at that time, was taken to be the zero shear stress position at which the smooth and rough surfaces were separated. Both profiles were used to calculate mean velocities and mean temperatures on each side of the zero shear surface and the temperature profile was transformed to give zero gradient at the zero shear surface rather than at the adiabatic wall. This procedure was followed for the majority of tests reported in Ref 2.

An alternative approach, the so-called Wilkie–White method[3–5], dispensed with the profiles but made use of the previously determined mean velocity and temperature correlations to calculate the ratios K_1, of mean densities and, K_2, of mean velocities. Additionally an empirical factor K_3, the ratio of transformed smooth wall friction factor in the rought/smooth annulus to the normal smooth pipe friction factor, was calculated. This factor was found to range from unity when facing surfaces were identical to typically 1.4 when a rough surface of practical interest faced a smooth surface. It was the first indication[2] of an error in the transformation when the maximum velocity surface was taken as the zero shear stress surface. Nevertheless the method worked quite well within and outside the limits of the correlations.

Steps were taken to check the assumption of coincidence of maximum velocity and zero-shear stress and it was found, by implication from friction factor measurements in rectangular channels with identical and non-identical roughness and by more direct measurements[7–9], that, as expected[7], the assumption is not exact. There is transfer of momentum across the maximum velocity surface so that the surface of zero shear stress is displaced towards the less rough wall. This displacement, although slight for transverse (or single-start) ribbed surfaces facing smooth surfaces, results in the transformed data for such roughened surface being estimated[4] to be about 10% too low on friction factor and about 1% too high on Stanton number, the values depending on the magnitude of the friction factor and Reynolds number of the roughened surface. The friction factor discrepancy is borne out by cluster measurements[10]. Adjustments can be made to the single pin data or the cluster predictions to offset the discrepancies.

Another approach is to adjust K_3 to a value closer to but greater than unity so that the zero shear surface is moved from its assumed position of coincidence with the maximum velocity surface towards its correct position displaced towards the smooth wall. Nathan and Pirie[11] and Warburton and Pirie[12] have presented values of K_3 aimed at producing transformed data based on the zero shear stress surface. A value of K_3 of 1.4 becomes 1.07. Thus even adopting the zero shear surface for isolating the opposing walls the drag on the smooth wall is increased by the presence of the smooth wall. The new K_3 values have been derived by several routes including measurements of drag on the smooth wall and measurements of shear stress distribution. There are consequent changes in K_2.

These methods use, as a basic measurement, the friction factor of the rough/smooth annulus. An alternative is to measure, additionally, the drag on the smooth wall by having a floating section or a Preston tube, for example. The results from such measurements tend to be scattered. An approach that should be more accurate, since the forces involves are very much longer, is to weigh the roughened pin with and without flow for two lengths of pin and by subtraction obtain the drag line for the difference in length[13], a technique which removes entry and exit effects.

Although the discrepancy between cluster pre-

* Heat Transfer and Fluid Flow Group, UKAEA, Windscale Nuclear Laboratories, Seascale, Cumbria CA20 1PF, UK
Received 30 January 1985 and accepted for publication in final form on 1 April 1985

diction and measurement is reduced by adopting the zero shear stress surface the method cannot be perfect. The reason is that the maximum velocity and zero shear stress surfaces coincide within a roughened cluster but not in an annulus. Even the pin weighing method would not be expected to give exact predictions. Moreover, passage shape can be expected to have an effect particularly for pin patch to diameter ratios below 1.2, if smooth tube data can be taken as a guide[14].

A check on the accuracy of the several methods is provided by cluster tests but some assumption on the effect of passage shape is required for closely packed clusters and for most clusters the ratio of roughness height to equivalent diameter varies within the cluster. Because of the presence of the smooth wall, a reverse transformation calculation is necessary for outer pins. Thus a particular cluster test will not readily distinguish uniquely between the methods. An approach that is more likely to be successful is to choose a particular array, square or triangular (since clusters are composed of one or the other or a mixture of both), and a particular pin pitch to diameter ratio, and measure the friction factor for an increasing number of pins in a smooth channel (friction factor is most affected by the transformation). The ratio of smooth to rough surface perimeter decreases with increasing number of pins and, by extrapolating the measured total friction factor to zero value of this ratio, the effect of the smooth wall is eliminated. The resultant value is the transformed friction factor for an infinite array of the chosen configuration and relative roughness height and with maximum velocity and zero shear stress surfaces coincident. The experiment can be repeated for a range of roughness heights and pin pitches and the results used for checking the existing transformation methods and modifying them if necessary.

Such a procedure has been followed here for square arrays of pitch-to-diameter ratio ranging from 1.04 to 1.76 and for pins of the same base diameter but three roughness heights. Measurements have been confined to friction factor. An alternative to extrapolation is to derive a transformed friction factor from the finite array results. The values obtained by these two different approaches are compared. Finally, single pins taken from the arrays and tested in a number of channels of different diameter have provided transformed friction factor data as a function of relative rib height at constant ratio of rib height to pin diameter for comparison with the values derived from the square array tests and for checking the single pin transformation methods.

Experiments

One metre long roughened pins with single-start ribs and a diameter of approximately 15 mm at the base of the ribs were chosen for the tests. They are the identical pins to those used for the tests in Ref 10. Three rib heights at a constant rib pitch to height ratio were studied. The dimensions and shapes are given in Table 1 and Fig 1. Each rib height quoted in the table is the mean of 240 measurements on 12 pins, the root diameter is the mean of 24 measurements on 4 pins and the rib pitch is the mean from 4 pins determined by a count of the number of complete pitches over an accurately measured distance of about 30 cm. Before the measurements were taken all pins had been shot-blasted to remove sharp corners from the ribs. The variations within and between pins of rib width, rib root radius, rib tip radius and rib pitch were not of sufficient magnitude to affect friction factor significantly[2]. In particular, rib tip radius has no effect once the sharpness has been removed as is the case for all surfaces tested. Rib height is the most important quantity. The effect of any variation is averaged out within pins by the large number of ribs (about 400) and between pins by the number of pins in a cluster for cluster tests but it is the main source of variation between pins in single pin tests.

Square arrays (Fig 2) with a pin pitch to pin base diameter ratio ranging from 1.04 to 1.76 were assembled (Table 2). For the 1.04 array the pins were close to

Notation

A	Total flow area
A_1	Flow area of sub-zone containing one-quarter of a pin
d	Untransformed equivalent diameter for single roughened pin in smooth circular channel or for square array of roughened pins in smooth square channel
d_1	Transformed equivalent diameter for single roughened pin or for infinite square array of roughened pins (for which case it is the same as the equivalent diameter of an inner sub-zone, type 1 of Appendix 1, in a finite square array)
D	Diameter of pin at rib foot
e	Height of rib
f	Untransformed friction factor
f_1	Transformed friction factor
K_1	Ratio of mean density outside the surface of zero shear stress to that inside
K_2	Ratio of mean velocity outside the surface of zero shear stress to that inside
K_3	Ratio of transformed smooth wall friction factor in a rough/smooth annulus to the normal smooth pipe friction factor
n	Number of pins in square array (Appendix 1), number of data points (Table 6)
p	Pitch of pins, ie distance between centres, in square array
$\Delta p/l$	Static pressure gradient
P	Total surface perimeter, $P_R + P_S$
P_1	Surface perimeter of a sub-zone containing one-quarter of a pin
P_R	Total perimeter of roughened pins, based on rib root diameter, in square array
P_S	Perimeter of smooth channel
Re	Untransformed Reynolds number but based on d_1, and hence becoming transformed Reynolds number for infinite square array
Re_1	Transformed Reynolds number
V	Mean gas velocity for whole passage
V_1, V_2, V_3	Velocities within sub-zones of types 1, 2, 3 respectively (Appendix 1)
ρ	Mean gas density

touching at the tips of the ribs. The distance between the smooth channel wall and the centres of the pins in the outer row was made equal to half the pin pitch. The number of pins in an array varied from 4 to 64. For the smaller arrays (36 pins or less) double length clusters were also tested to check that the single length was adequate. The length to equivalent diameter ratio of the clusters ranged from 170 to 22 for the single length assemblies. Three roughness heights were chosen, resulting in ratios of roughness height to equivalent diameter calculated for the fully roughened region, ranging from 0.005 to 0.055 (Table 2). Measurements of the width and breadth (or rather height, since the channel was horizontal) of the smooth channel were made at a number of planes. One such set is given in Table 3. The smooth channel was formed from four steel plates for the tests with $p/D = 1.76$. For all other tests only the bottom plate was retained, the other three being perspex plates inserted into the channel to reduce the size for the smaller pitch-to-diameter ratios. The surface finish of the plates is given in Table 4. Twenty-two pressure tappings (11 for each cluster) were located 7.5 cm apart along the centre line of the bottom plate and static pressures were measured on banks of water manometers. Tests were carried out with air at slightly above ambient pressure and temperature. Flowrates were measured by a calibrated orifice meter. Reynolds numbers were in the range 5000 to 10^5, the values depending on p/D. Thus for $p/D = 1.04$, Re ranged from 5000 to 1.2×10^4 and for $p/D = 1.76$, Re ranged from 4×10^4 to 10^5.

Single pins were chosen from the total batch used for building the arrays and tested in several channels of diameter ranging from 19.3 mm to 51.3 mm (Table 5) in order to provide the transformed friction factor data for comparison with the cluster results. The experimental

Table 1 Dimensions of roughened pins

Type	Pin diameter at base of roughness D, mm	Mean roughness height e mm	$e/D \times 10^3$	Rib pitch / Rib height
9	15.316	0.2263	14.8	7.27
11	15.304	0.2774	18.1	7.30
13	15.291	0.3294	21.5	7.23

Note: Types 9, 11 and 13 were used in Ref 10 and have nominal rib heights of 0.009, 0.011 and 0.013 in respectively

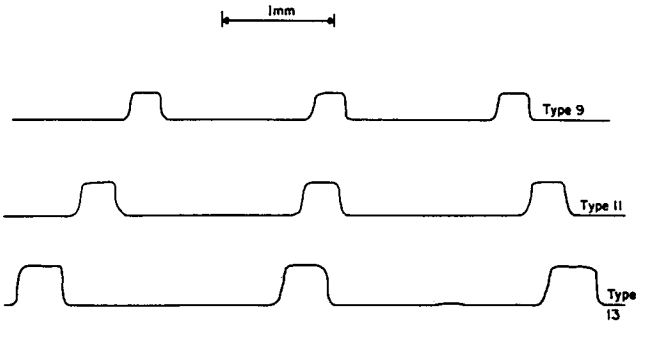

Fig 1 Typical rib profiles

Table 2 Geometrical parameters of square arrays

$\frac{p}{D}$	Ratio of rib height to equivalent diameter, $e/d_1 \times 10^3$, for pins of type:–		
	9	11	13
1.046	37.9	46.0	54.6
1.099	27.6	33.7	39.9
1.149	21.8	26.7	31.6
1.202	17.7	21.6	25.6
1.251	14.9	18.2	21.6
1.402	–	12.0	–
1.763	5.01	6.13	7.27

$\frac{p}{D}$ = pin pitch / mean pin diameter (15.304 mm)

d_1 = equivalent diameter within the fully roughened zone of a square array based on actual pin diameter

For p/D = 1.402 no tests were carried out with pins of types 9 and 13

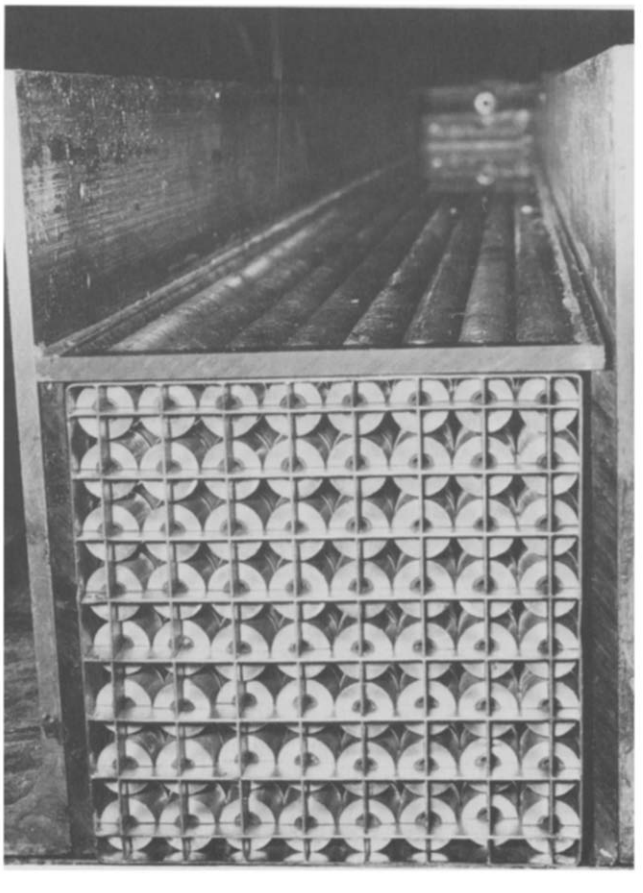

Fig 2 General view of square array, $p/D = 1.04$

Table 3 Dimensions of channel for all tests with 4× 4 array at p/D= 1.25

Height, mm		Width, mm	
One-side	Other side	Bottom	Top
Downstream cluster position			
76.581	76.810	76.784	77.343
76.606	76.733	76.759	77.216
76.581	76.733	76.810	77.343
76.556	76.657	77.089	77.597
76.581	76.733	77.013	77.572
76.606	76.708	76.835	77.495
76.581	76.657	76.886	77.470
76.632	76.606	77.038	77.343
76.708	76.581	77.114	77.419
76.708	76.606	77.089	77.394
76.810	76.606	77.038	77.318
	Mean 76.657		77.216
Area= 5919.2 mm²			
Upstream cluster position			
76.759	76.632	77.064	77.394
76.784	76.556	76.886	77.394
76.759	76.606	76.810	77.470
76.733	76.632	76.886	77.521
76.810	76.708	76.835	77.597
76.835	76.632	76.810	77.648
76.810	76.606	76.886	77.673
76.810	76.606	76.937	77.597
76.759	76.632	76.911	77.648
76.835	76.632	76.937	77.724
76.759	76.581	76.886	77.749
	Mean 76.708		77.241
Area= 5925.0 mm²			

These measurements are at tapping positions starting with the position nearest the outlet

Table 4 Surface finish of channel plates

	μm CLA
Steel plate	0.40 (with some spots up to 4.0)
Perspex plate	0.025 to 0.040

arrangement and technique were similar to that for the cluster work except that only a single length was tested, the pressure tappings were a minimum of 8 in number and a pressurised rig was used for the tests in the smallest channel.

Results

An example of the variation in static pressure along a channel is shown in Fig 3. From lines such as this, the friction factor of the square array within its smooth channel has been calculated. Plots of these untransformed friction factors against untransformed Reynolds numbers are presented in Fig 4 for one value of p/D. Friction factor is seen to be independent of Reynolds number. Thus it has not been necessary to apply corrections for differences in Reynolds number between the tests. (In any case for a given p/D a common Reynolds number can be chosen for any size of array, eg 7×10^4). The mean friction factor for

Table 5 Dimensions of circular channels for single pin tests

Diameter, mm	19.253	21.641	26.670	32.944	51.308
Surface finish, μm CLA	0.08	–	0.30	0.22	–

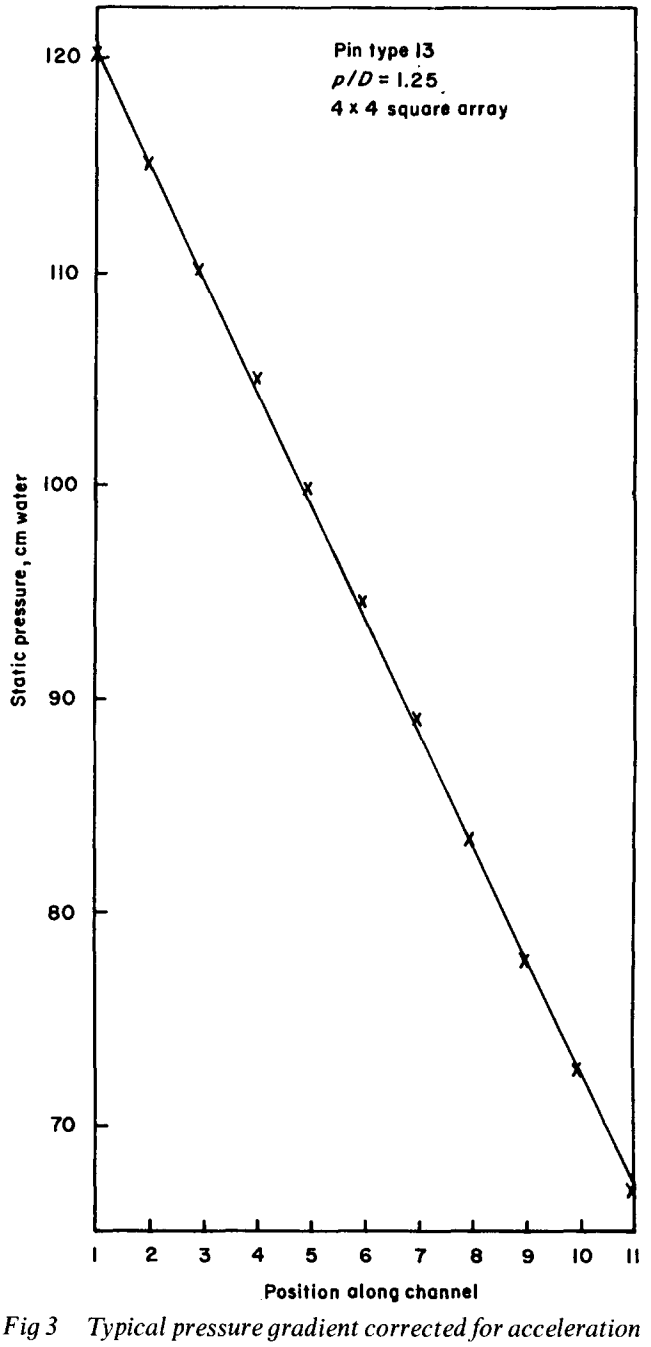

Fig 3 Typical pressure gradient corrected for acceleration

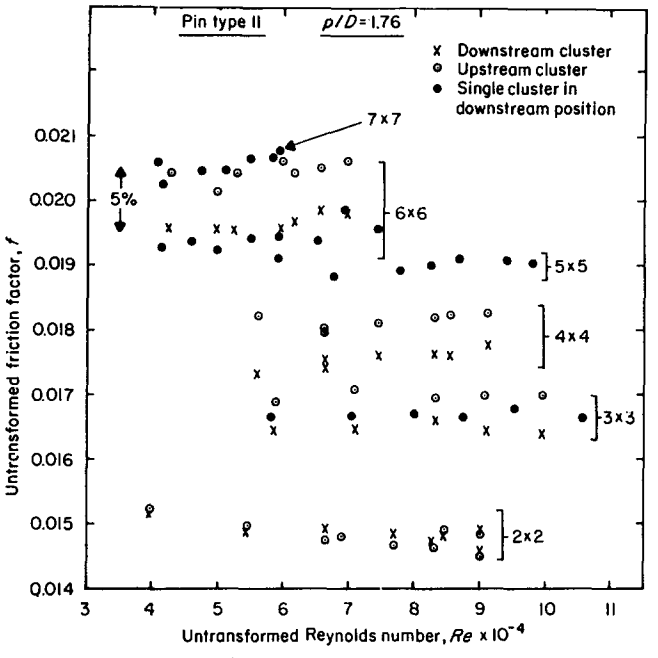

Fig 4 Variation of untransformed friction factor with untransformed Reynolds number for $p/D = 1.76$

each cluster has been calculated and plotted as a function of rough and smooth perimeter (eg Fig 5). The more obvious plot against the ratio of smooth to rough perimeter results in a series of curves making extrapolation to zero value of this ratio difficult. The curvature arises from the proximity of the smooth wall, which, being located only half a pitch from the outer pins causes the zero shear stress surface to be closer to the pins in the outer zone than it is in the body of the cluster. Thus the friction factor for a significant portion of the cluster, namely the outer halves of the outer pins, is inflated. This inflation is greater for smaller arrays and tends to zero when the perimeter ratio tends to zero. When the ratio of rough to total perimeter is chosen for the abscissa a series of straight lines is obtained leading to simple and accurate extrapolation to unit value of this ratio. Proof of linearity is given in Appendix 2.

The friction factors obtained by extrapolation of the least squares fitted lines correspond to transformed friction factors but with the maximum velocity and zero shear surfaces coincident. They are presented in Table 6 and Fig 6.

An alternative route to extrapolation is to calculate the transformed or inner sub-zone friction factor from the square array results. This has been done (see Appendix 1) without making use of one or other of the usual set of assumptions required for the transformation of single pin friction factors. The only assumptions that need to be made are that the pressure gradient is the same in all sub-zones and that the relative velocities in the sub-zones are independent of the number of pins in the array. The measured friction factors for 2×2, 5×5 and 8×8 arrays were derived from the best straight lines fitted to the data represented by Fig 5 and substituted into the equations in Appendix 1 to derive the transformed friction factors and the velocity ratios (linearity is not a pre-requisite of the method).

The close agreement between the extrapolated and calculated transformed friction factors (Table 6) lends support to the validity of the assumptions adopted.

The velocity ratios are listed in Table 7. Whereas the velocity in an outer non-corner sub-zone is some 10% below that of an inner sub-zone, that in an outer corner zone is half as much again below.

Single pin transformed friction factors for 2 pins of type 11 are potted as a function of log *Re* for 5 channel diameters in Fig 7. The indications are that there is no effect of Reynolds number although the range is small. Mean values have been taken and are plotted in Fig 8 as a function of e/d_1 (at constant e/D) using 3 transformation methods. On the same graph the square array results for type of pin have been reproduced from Fig 6 for comparison.

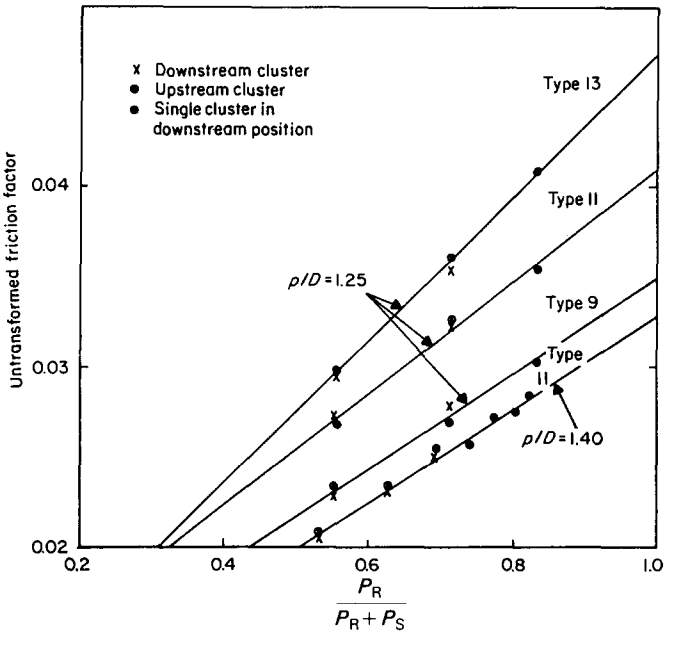

Fig 5 Square array results for $p/D = 1.24$ and 1.40

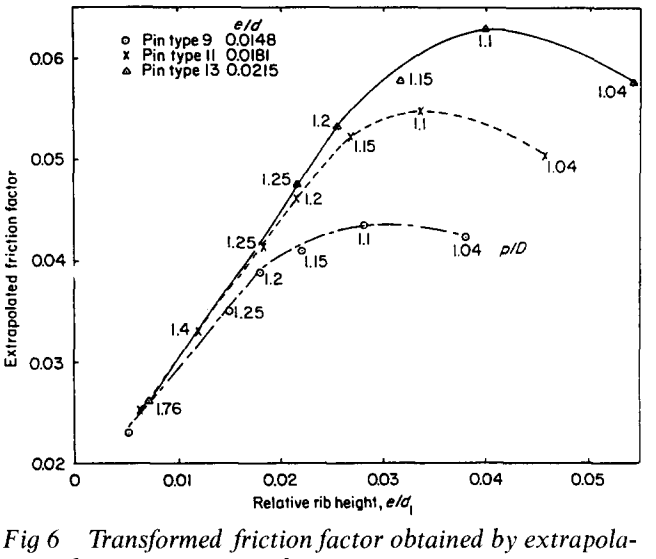

Fig 6 Transformed friction factor obtained by extrapolation of square array results

Table 6 Transformed friction factors derived from square array results

P/D	Pin type 9					Pine type 11					Pin type 13				
	e/d_1 $\times 10^3$	n	$f_1 \times 10^3$ extrap	95% confd. limits %	$f_1 \times 10^3$ Calc	e/d_1 $\times 10^3$	n	$f_1 \times 10^3$ extrap	95% confd. limits %	$f_1 \times 10^3$ Calc	e/d_1 $\times 10^3$	n	$f_1 \times 10^3$ extrap	95% confd. limits %	$f_1 \times 10^3$ Calc
1.04	37.9	5	42.05	6.8	42.05	46.2	11	50.39	1.4	50.39	54.6	5	57.85	5.1	57.85
1.10	27.6	5	43.67	7.4	43.68	33.7	5	54.85	17.3	54.88	39.9	5	63.15	6.1	63.14
1.15	21.8	5	40.59	9.0	40.56	26.7	5	52.32	3.0	52.33	31.6	5	57.78	7.2	57.74
1.20	17.7	5	38.72	12.2	38.73	21.6	5	46.24	4.5	46.24	25.6	5	53.38	3.2	53.38
1.25	14.9	5	35.09	5.7	35.09	18.2	5	41.40	4.6	41.45	21.6	5	47.61	3.5	47.61
1.40	–	–	–	–	–	12.0	10	33.26	2.2	33.27	–	–	–	–	–
1.76	5.01	3	23	84	23.42	6.13	12	25.22	3.1	25.25	7.27	3	26.09	12.8	26.12

n= number of points determining the straight line from which f_1 is obtained by extrapolation

Table 7 Square array sub-zone velocity ratios

	Pin type 9			Pin type 11			Pin type 13		
P/D	V_2/V_1	V_3/V_1	$\frac{1-V_3/V_1}{1-V_2/V_1}$	V_2/V_1	V_3/V_1	$\frac{1-V_3/V_1}{1-V_2/V_1}$	V_2/V_1	V_3/V_1	$\frac{1-V_3/V_1}{1-V_2/V_1}$
1.04	0.918	0.871	1.58	0.987	0.974	2.00	0.933	0.890	1.64
1.10	0.906	0.855	1.54	0.910	0.857	1.59	0.936	0.895	1.64
1.15	0.881	0.835	1.38	0.921	0.869	1.65	0.920	0.879	1.52
1.20	0.952	0.915	1.77	0.932	0.888	1.65	0.960	0.930	1.76
1.25	0.903	0.854	1.51	0.909	0.853	1.61	0.938	0.896	1.68
1.40	–	–	–	0.914	0.861	1.60	–	–	–
1.76	0.875	0.822	1.42	0.882	0.825	1.49	0.854	0.802	1.36

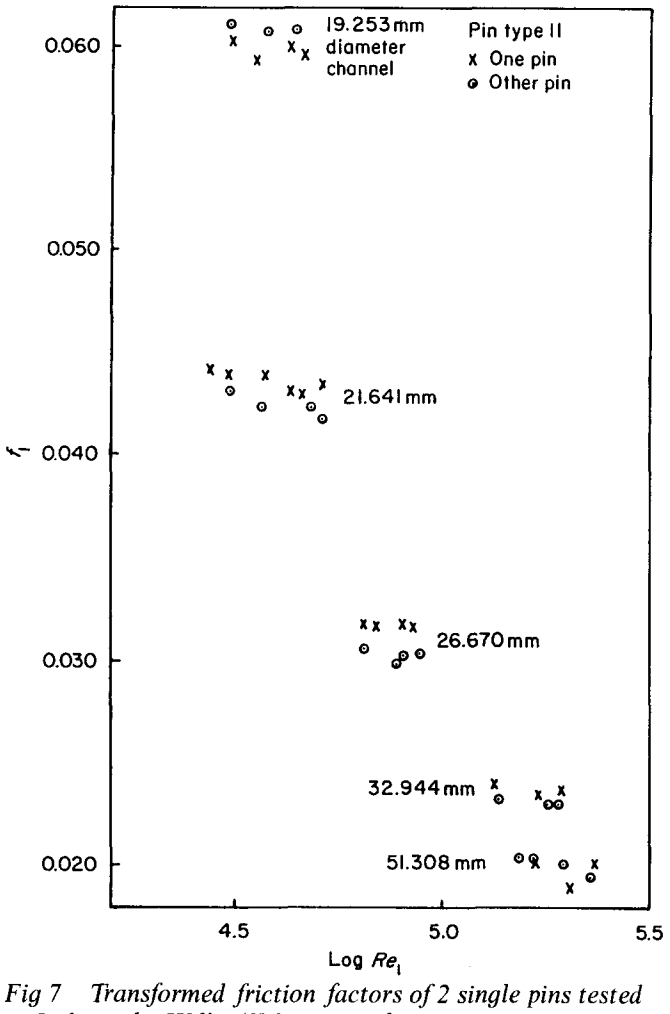

Fig 7 Transformed friction factors of 2 single pins tested in 5 channels, Wilkie/White transformation

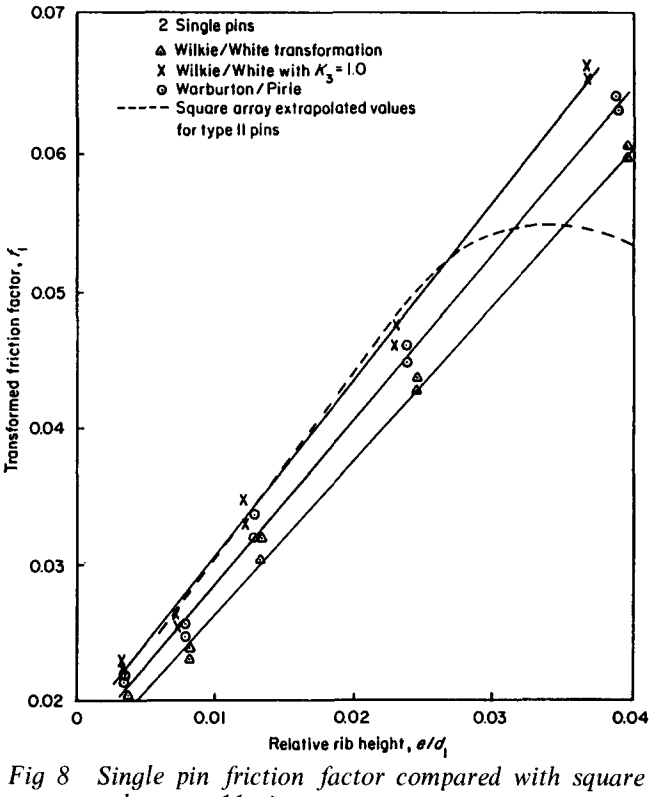

Fig 8 Single pin friction factor compared with square array results, type 11 pins

Discussion

The square array results (Fig 6) reveal a difference in friction factor for the three types of pin. This may be due either to differences in rib profile, although Fig. 1 indicates that this is rather unlikely, or to differences in rib height to pin diameter e/D, a parameter that has been shown by

Lee[15] to have some effect. The latter variable no doubt accounts for the large effect at low values of p/D. For $p/D = 1.04$ the rib tips touch at the highest e/D but leave a gap at the lower values. At the low values of e/d_1 (<0.01) in the usual range of reactor interest there is no effect of e/D over the range covered.

Friction factor varies linearly with e/d_1 until values of p/D less than 1.2 are reached. The close pitching results in excessive distortion of the passage shape and the breakdown in the equivalent diameter concept. The critical value, just under 1.2, seems to be independent of e/D, and is in rough agreement with that for smooth pin arrays[14,16]. It is interesting to note from Fig 6 that points of fixed p/D lie on straight lines of roughly similar slope so that only the intercept on the ordinate is appreciably affected by p/D. The data, which cover an extensive range of e/d_1 and p/D are of value for calculations involving bowed and displaced pins.

The single pin friction factor at constant e/D varies linearly with e/d_1 over the full range (Fig 8 for pin type 11), even although the rib-tip to channel wall clearance is as small as 1.7 mm for the highest e/d_1. There is agreement with the square array results over the linear range. Worst agreement is obtained, not unexpectedly, using the Wilkie/White transformation. The discrepancy of about 12% at a value of e/d_1 pf 0.007 conforms with current views. Best agreement is obtained using the Wilkie/White transformation but with K_3 equal to unity. However, the Warburton/Pirie transformation, although giving lower results everywhere is not significantly different mainly because of the scatter on the single pin tests. The need for further such tests is evident. The equations for friction factor for $e/D = 0.0181$ are:

$$f_1 = 0.01735 + 1.314 e/d_1 \quad \text{(Wilkie/White } K_3 = 1\text{)}$$

$$f_1 = 0.01678 + 1.204 e/d_1 \quad \text{(Warburton/Pirie)}$$

The equation for the corresponding square array over the linear range is:

$$f_1 = 0.01695 + 1.352 e/d_1$$

The data of Lee[15] for constant e/D (surface 2) and varying e/d_1 transformed by the Nathan/Pirie method is in good agreement with the present single pin data transformed by the closely similar Warburton/Pirie method.

A single pin test in a concentric circular channel cannot provide specific information on passage distortion effects. To predict such effects from concentric single pin data requires some considerable modification of current calculation methods. An alternative route might be to utilise eccentric annulus data.

The fact that the Warburton/Pirie method appears to give a lower friction factor is to be expected from the non-coincidence of the zero shear and maximum velocity surfaces in the annulus. Moreover, since the roughened surface increases the friction factor of the smooth surface (as indicated by K_3 being greater than unity) it is evident that the smooth surface will decrease the friction factor of the roughened surface.

Thus there are 3 routes open for making an accurate prediction of cluster friction factor:

- Adopting a transformation method based on the maximum velocity surface (eg Hall, Wilkie/White) and then making an adjustment to obtain agreement with cluster results.
- Adopting a transformation method based on the zero shear surface (eg Warburton/Pirie) and hence giving the true shear stress for the pin but for an unrealistic velocity distribution and then making an adjustment to obtain agreement with cluster results.
- Adopting a transformation method that gives the cluster friction factor without the need for adjustment (eg Wilkie/White with $K_3 = 1$). This method implies that the boundary separating the rough and smooth zones is at a greater distance from the maximum velocity surface than is the zero shear stress surface.

The problem is to determine which, if any of these routes is universally applicable bearing in mind that the adjustments are empirically based or, if none, which gives or is likely to give the closest prediction most frequently. The present work and that of Wilson *et al.*[13] tend to favour the third route.

Conclusions

From friction factor measurements on square arrays of roughened pins of varying pin pitch to pin diameter ratio and rib height to pin diameter ratio and on single roughened pins in smooth channels of varying diameter it can be concluded that, with reference to transformed friction factors:

(a) Pin pitch to diameter ratio has no effect until values below 1.2 are reached, in conformity with published data on smooth arrays.
(b) Rib height to pin diameter ratio has little effect, over the range studied, for low relative rib heights but a large effect at high relative rib heights and low pin pitch to diameter ratios.
(c) Relative rib height, e/d_1, produces a linear increase (until pin pitch to diameter effects operate) both for square arrays and single pins.
(d) Single pin data transformed by the Wilkie/White method but modified by putting K_3 equal to unity gives the best agreement with the square array results, whereas the Warburton/Pirie method gives results about 7% low, but the result is not statistically significant owing to insufficient number of tests on single pins.

References

1. **Hall W. B.** Heat transfer in channels composed of rough and smooth surfaces. *UKAEA IGR-TN/W-832 (1958), also J. Mech. Eng. Sci. (Sept. 1962)*
2. **Wilkie D.** Forced convection heat transfer from surfaces roughened by transverse ribs. *Third Int. Heat Transfer Conf., Chicago 1966, Paper No. 1*
3. **Wilkie D.** Calculation of heat transfer and flow resistance of rough and smooth surfaces contained in a single passage. *Third Int. Heat Transfer Conf., Chicago 1966, Paper No. 2*
4. **Wilkie, D.** Calculation of heat transfer and flow resistance of rough and smooth surfaces contained in a single passage. *EAES Heat Transfer Symposium on Superheated Steam and Gas, Bern 1966*
5. **Wilkie D. and White L.** Calculation of flow resistance of passages bounded by a combination of rough and smooth surfaces. *UKAEA TRG Report 1113(W), 1965, also JBNES, January 1967*
6. **Wilkie D, Cowin M., Burnett P. and Burgoyne T.** Friction factor measurements in a rectangular channel with walls of identical and non-identical roughness. *Int. J. Heat and Mass Transfer*, **10** *(May 1967), 611–621, also TRG Report 539(W), 1963*

7. **Kjellstrom B. and Hedberg S.** On shear stress distributions for flow in smooth or partially rough annuli. *AE-RTL-796 (1965)*
8. **Stephens M. J.** Investigation of flow in a concentric annulus with smooth outer wall and rough inner wall, Part 1 Transverse rib type roughnesses. *CEGB Report RD/B/N1535 (1970)*
9. **Hanjalic K. and Launder B. E.** Fully developed flow in rectangular ducts of non-uniform surface texture. I. An experimental investigation. *Imperial College TWF/TN/48 (1968)*
10. **White L. and White W. J.** Comparison of 36-rod cluster pressure drop measurement with prediction using data obtained from single rods. *Symposium on subsonic flow losses in complex passages and ducts. IME London 4–5 October 1967, Paper No. 6*
11. **Nathan D. I. and Pirie M. A. M.** On the interpretation of heat transfer and pressure drop tests on roughened rods in smooth circular channels. *CEGB Report RD/B/N1370 (1970)*
12. **Warburton C and Pirie M. A. M.** An improved method for analysing heat transfer and pressure drop tests on roughened rods in smooth channels. *CEGB Report RD/B/N2621 (1973)*
13. **Wilson J. T., Jackson G and Fletcher D. J.** A direct measurement of the friction factor of roughened surfaces. *NEA Heat Transfer Specialist Meeting, Petten. 17–19 September 1975*
14. **Redman J. D., McKee G. and Rule I. C.** The influence of flux distribution and surface temperature distribution on turbulent forced convective heat transfer in clusters of tubes in which the flow of coolant is parallel to the axes of the tubes. *Third Int. Heat Transfer Conf.*, Chicago 1966, Paper No. 19
15. **Lee C. J.** Investigation of flow parameters for a series of concentric rough pin and smooth channel assemblies. *EUB Report RD/B/N2404 (Sept. 1972)*
16. **Marek J., Maubach K. and Rehme K.** Heat transfer and pressure drop performance of rod bundles arranged in square arrays. *Int. J. Heat Mass Transfer*, **16** *(1973), 2215–2228*

APPENDIX 1: Calculation of transformed friction factor from several square array tests

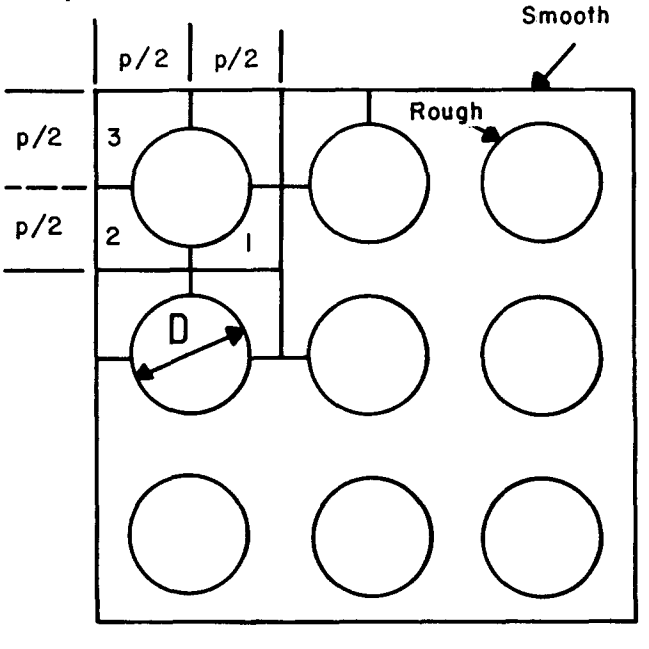

Fig A.1 Square array n = 3

Consider a square array with n pins along each side (Fig A.1) divided into sub-zones each containing $\frac{1}{4}$ of a roughened pin. There are:

$(2n-2)^2$ sub-zones of type 1 which have no smooth surface

$4(2n-2)$ sub-zones of type 2 which have $p/2$ smooth surface perimeter

4 sub-zones of type 3 which have p smooth surface perimeter

Assuming the same pressure gradient for every sub-zone:

$$\frac{\Delta p}{1}=\frac{4f}{d}\frac{1}{2}\rho V^2=\frac{4f_1}{d_1}\frac{1}{2}\rho V_1^2 \tag{1}$$

where f and d refer to the untransformed friction factor and equivalent diameter respectively, ρ and V refer to the mean density and velocity for the whole passage and suffix 1 refers to the inner sub-zone and hence transformed values. From Eq (1):

$$\frac{f_1}{f}=\frac{d_1}{d}\left(\frac{V}{V_1}\right)^2 \tag{2}$$

Since all sub-zones are of equal area:

$$V=\frac{(2n-2)^2V_1+4(2n-2)V_2+4V_3}{4n^2}$$

where V_2 and V_3 are the mean velocities in sub-zones 2 and 3. Thus:

$$\frac{V}{V_1}=\left(\frac{n-1}{n}\right)^2+\frac{2n-2}{n^2}\frac{V_2}{V_1}+\frac{1}{n^2}\frac{V_3}{V_1} \tag{3}$$

Also:

$$\frac{d_1}{d}=\frac{A_1}{A}\frac{P}{P_1}$$

where total area $A=4n^2A_1$, $P_1\,(=\pi D/4)$ is the perimeter of an inner sub-zone and $P\,(=4np+4n^2\pi D/4)$ is the total passage perimeter. Therefore:

$$d_1/d=\frac{4n^2\pi D/4+4np}{4n^2\pi D/4}=1+\frac{4p/D}{n\pi}=\frac{P}{P_R} \tag{4}$$

where P_R is the total roughened perimeter in square array. Substituting Eqs (3) and (4) in (2) gives:

$$f_1f=\frac{P}{P_R}\left[\left(\frac{n-1}{n}\right)^2+\frac{2n-2}{n^2}\frac{V_2}{V_1}+\frac{1}{n^2}\frac{V_3}{V_1}\right]^2 \tag{5}$$

from which it can be seen that as $n\to\infty$, $f\to f_1$ as expected. Eq (5) possesses 3 unknowns f_1, V_2/V_1 and V_3/V_1. It is reasonable to assume that the 2 velocity ratios are independent of n. Adjacent sub-zones of different type may be expected to influence each other (eg sub-zone 3 may reduce the velocity of the adjacent sub-zone 2) but any effect is likely to be small and will diminish in importance as n increases. Invoking the proposed assumption and substituting 3 values of n and the corresponding measured values of f into Eq (5) results in 3 equations which can be solved to give:

$$\frac{9}{f_1^{1/2}}=\frac{32}{\left(f\frac{P}{P_R}\right)_{n=8}^{1/2}}-\frac{25}{\left(f\frac{P}{P_R}\right)_{n=5}^{1/2}}+\frac{2}{\left(f\frac{P}{P_R}\right)_{n=2}^{1/2}} \tag{6}$$

$$\frac{V_2}{V_1}=\frac{16}{3}\left(\frac{f_1}{\left(f\frac{P}{P_R}\right)_{n=8}}\right)^{1/2}-\frac{1}{3}\left(\frac{f_1}{\left(f\frac{P}{P_R}\right)_{n=2}}\right)^{1/2}-4 \tag{7}$$

$$\frac{V_3}{V_1}=4\left(\frac{f_1}{\left(f\frac{P}{P_R}\right)_{n=2}}\right)^{1/2}-2\frac{V_2}{V_1}-1 \tag{8}$$

APPENDIX 2: Proof that measured friction factor is a linear function of perimeter ratio

From Eq (5) of Appendix 1:

$$\frac{f}{f_1}=\frac{P_R}{P}\left[\left(\frac{n-1}{n}\right)^2+\frac{2n-2}{n^2}\frac{V_2}{V_1}+\frac{1}{n^2}\frac{V_3}{V_1}\right]^{-2}$$

which reduces to:

$$\frac{f}{f_1}=\frac{P_R}{P}\left(1-\frac{2}{n}X+\frac{1}{n^2}Y\right)^{-2}$$

where $X=1-V_2/V_1$ and $Y=2(1-V_2/V_1)-(1-V_3/V_1)$. Binomial expansion gives:

$$f/f_1=\frac{P_R}{P}\left[1+\frac{4}{n}X+\frac{2}{n^2}(6X^2-Y)+\frac{4}{n^3}(8X^3-3XY)+\cdots\right]$$

Values of X and Y supplied by the data in Table 7 show that the cubic term in n is negligible and the quadratic term is quite small. Even for $n=2$ it is less than 1% in all cases. Therefore:

$$f/f_1=\frac{P_R}{P}\left[1+\frac{4}{n}X\right]$$

$$=\frac{P_R}{P}\left[1+\frac{\pi}{p/D}\left(1-\frac{V_2}{V_1}\right)\left(\frac{P}{P_R}-1\right)\right]$$

using Eq (4). Therefore:

$$f=a+b\frac{P_R}{P}$$

where:

$$a=\frac{f_1\pi}{p/D}\left(1-\frac{V_2}{V_1}\right)$$

and

$$b=f_1\left[1-\frac{\pi}{p/D}\left(1-\frac{V_2}{V_1}\right)\right]$$

where V_2/V_1 and f_1 are constant for a given value of p/D.

BOOK REVIEW

Flow Visualization III

Ed. W-J Yang

This volume is a collection of papers presented at the Third International Symposium on Flow Visualization, held in Michigan in September 1983. Like the two previous collections in this series, this one contains a wealth of information pertinent to the techniques for rendering flows visible and the applications thereof.

I found it particularly useful by virtue of its international orientation. Recent international developments in this field, particularly by the Japanese, are well represented here even though they do not often appear in the usual American and European archival journals.

The volume also serves to indicate what are the current directions of the state-of-the-art in flow visualization. Thus, while traditional methods and applications are well represented, substantial sections are also devoted to such topics as laser-based techniques, image processing, computer-generated graphics, and biomedical applications.

The volume contains 157 papers of which seven are invited lectures. The major categories of flow visualization applications covered are: separated flows, vortices and wakes, supersonic flows and shock waves, jets, internal flows, stratified and boundary layer flows, rheology, ships and waves, aerodynamocs, atmospherics and oceanography, fluid machinery, heat transfer, and combustion. The high quality of the published illustrations is especially noteworthy.

In summary, this book is a valuable resource for anyone who practices flow visualization in particular, as well as for the fluid mechanics community in general.

Gary S. Settles
The Pennsylvania State University,
PA, USA

Published price $95.00 by Hemisphere Publishing Corporation, 79 Madison Avenue, New York, NY 10016, USA. Springer-Verlag, Heidelberger Platz 3, Postfach, D-1000 Berlin 33, FRG